

ISSN: (Print) (Online) Journal homepage: <https://www.tandfonline.com/loi/tbsd20>


Novel inhibitors with sulfamethazine backbone: synthesis and biological study of multi-target cholinesterases and α -glucosidase inhibitors

Cüneyt Türkeş, Suleyman Akocak, Mesut Işık, Nebih Lolak, Parham Taslimi, Mustafa Durgun, İlhami Gülçin, Yakup Budak & Şükrü Beydemir


To cite this article: Cüneyt Türkeş, Suleyman Akocak, Mesut Işık, Nebih Lolak, Parham Taslimi, Mustafa Durgun, İlhami Gülçin, Yakup Budak & Şükrü Beydemir (2022) Novel inhibitors with sulfamethazine backbone: synthesis and biological study of multi-target cholinesterases and α -glucosidase inhibitors, Journal of Biomolecular Structure and Dynamics, 40:19, 8752-8764, DOI: [10.1080/07391102.2021.1916599](https://doi.org/10.1080/07391102.2021.1916599)

To link to this article: <https://doi.org/10.1080/07391102.2021.1916599>

 View supplementary material [↗](#)

 Published online: 05 May 2021.

 Submit your article to this journal [↗](#)

 Article views: 678





 View related articles [↗](#)

 View Crossmark data [↗](#)

 Citing articles: 25 View citing articles [↗](#)



Novel inhibitors with sulfamethazine backbone: synthesis and biological study of multi-target cholinesterases and α -glucosidase inhibitors

Cüneyt Türkeş^a , Suleyman Akocak^b, Mesut Işık^c, Nebih Lolak^b, Parham Taslimi^d , Mustafa Durgun^e , İlhami Gülçin^f , Yakup Budak^g and Şükrü Beydemir^{h,i}

^aDepartment of Biochemistry, Faculty of Pharmacy, Erzincan Binali Yıldırım University, Erzincan, Turkey; ^bDepartment of Pharmaceutical Chemistry, Faculty of Pharmacy, Adıyaman University, Adıyaman, Turkey; ^cDepartment of Bioengineering, Faculty of Engineering, Bilecik Şeyh Edebali University, Bilecik, Turkey; ^dDepartment of Biotechnology, Faculty of Science, Bartın University, Bartın, Turkey; ^eDepartment of Chemistry, Faculty of Arts and Sciences, Harran University, Şanlıurfa, Turkey; ^fDepartment of Chemistry, Faculty of Sciences, Atatürk University, Erzurum, Turkey; ^gDepartment of Chemistry, Faculty of Arts and Sciences, Gaziosmanpaşa University, Tokat, Turkey; ^hDepartment of Biochemistry, Faculty of Pharmacy, Anadolu University, Eskişehir, Turkey; ⁱThe Rectorate of Bilecik Şeyh Edebali University, Bilecik, Turkey

Communicated by Ramaswamy H. Sarma

ABSTRACT

The underlying cause of many metabolic diseases is abnormal changes in enzyme activity in metabolism. Inhibition of metabolic enzymes such as cholinesterases (ChEs; acetylcholinesterase, AChE and butyrylcholinesterase, BChE) and α -glucosidase (α -GLY) is one of the accepted approaches in the treatment of Alzheimer's disease (AD) and diabetes mellitus (DM). Here we reported an investigation of a new series of novel ureido-substituted derivatives with sulfamethazine backbone (**2a-f**) for the inhibition of AChE, BChE, and α -GLY. All the derivatives demonstrated activity in nanomolar levels as AChE, BChE, and α -GLY inhibitors with K_i values in the range of 56.07–204.95 nM, 38.05–147.04 nM, and 12.80–79.22 nM, respectively. Among the many strong *N*-(4,6-dimethylpyrimidin-2-yl)-4-(3-substituted-phenylureido) benzenesulfonamide derivatives (**2a-f**) detected against ChEs, compound **2c**, the 4-fluorophenylureido derivative, demonstrated the most potent inhibition profile towards AChE and BChE. A comprehensive ligand/receptor interaction prediction was performed *in silico* for the three metabolic enzymes providing molecular docking investigation using Glide XP, MM-GBSA, and ADME-Tox modules. The present research reinforces the rationale behind utilizing inhibitors with sulfamethazine backbone as innovative anticholinergic and antidiabetic agents with a new mechanism of action, submitting propositions for the rational design and synthesis of novel strong inhibitors targeting ChEs and α -GLY.

ARTICLE HISTORY

Received 4 March 2021
Accepted 8 April 2021





KEYWORDS


Acetylcholinesterase; butyrylcholinesterase; α -glucosidase; sulfamethazine; *in silico* study

1. Introduction

Neurons are unparalleled among cell species in mammalian organisms for their characteristic variety of secretory complexes and their heterogeneity in size and shape. Acetylcholine (ACh) was discovered due to the determination that the inhibitory nerves released a substance inhibiting the heart's chronotropic. Discovered by Loewi as a result of research done with isolated heart preparations in the early 1920s, ACh is the first known neurotransmitter (Pohanka, 2012). It has functions in the peripheral and central nervous system such as attention (Istrefi et al., 2020), motivation (Collins et al., 2016), arousal (Ruivo et al., 2017), memory (Işık et al., 2020c), learning (Provinsi et al., 2020), and activate muscles (Benham et al., 1985). People with Alzheimer's disease (AD) have reduced levels of ACh in the brain (Francis, 2005). The only clear case of a transmitter known to be inactivated by the extracellular enzymes is ACh. The enzymes

responsible for the break-down of ACh are cholinesterases (ChEs), i.e. acetylcholinesterase (EC 3.1.1.7; acetylcholine hydrolase, AChE) and butyrylcholinesterase (EC 3.1.1.8; acylcholine acylhydrolase, BChE) (Krieger, 2010). On the other hand, AChE is more specific for ACh than BChE (Reale et al., 2018). These enzymes, which possess in various tissues, neurons, and the surrounding extracellular space (Işık et al., 2017), in many species, including humans, are hydrolyzing the quaternary amine ACh to choline (Ch) and acetic acid within milliseconds (Kessler et al., 2017). However, it remains the capacity of BChE to hydrolyze higher Ch esters, such as butyrylcholine, is a significant physiological function of this enzyme (Chuiko, 2000). ChE inhibitors (ChEIs) increase ACh levels by inhibiting the action of AChE and BChE, which are accountable for the breakdown of ACh (Taslimi et al., 2020a). The main use of ChEIs is for the therapy of dementia in patients with AD (Işık, 2019). While numerous ChEIs, in

CONTACT Cüneyt Türkeş  cuneyt.turkes@erzincan.edu.tr  Department of Biochemistry, Faculty of Pharmacy, Erzincan Binali Yıldırım University, Erzincan, 24100, Turkey; Suleyman Akocak  sakocak@adiyaman.edu.tr  Department of Pharmaceutical Chemistry, Faculty of Pharmacy, Adıyaman University, Adıyaman, 02040, Turkey

 Supplemental data for this article can be accessed online at <https://doi.org/10.1080/07391102.2021.1916599>.

particular, such as donepezil, galantamine, neostigmine, physostigmine, rivastigmine, tacrine are available (Kilic et al., 2020; Mughal et al., 2018; Zaman et al., 2019), tend to reason potentially serious side effects (Mughal et al., 2019), such as vasodilation, slow heart rate, weight loss, constriction of the respiratory tract, constriction of the pupils in the eyes (Schneider, 2000).

It is known that there is a possible relationship between neurodegenerative AD and type 2 diabetes mellitus (DM). Studies in recent years have focused on systems that control synaptic and neuronal functions in the brain. It has been determined that insulin controls synaptic and neuronal functions in the brain. Also, it has been determined that DM patients are more likely to have AD and dementia. In the light of this information, the reason why DM is associated with AD has been expressed as follows; The defect in insulin secretion may be responsible for forming both diseases (Han & Li, 2010). In other words, its deficiency or elevated levels can cause AD and DM. Furthermore, ChE enzymes are known to be associated with diabetes. In a study conducted for this purpose, AChE activity has been higher in streptozotocin-induced diabetic rats than in control groups. Moreover, BChE activity was significantly increased in type 1 and type 2 DM compared to control groups (Abbott et al., 1993). These results imply that inhibition of cholinesterase enzymes could be important for treating DM, as in AD patients.

One of the important therapeutic approaches to be considered in DM may be possible with the inhibition of carbohydrate hydrolyzing enzymes such as α -glucosidase (EC 3.2.1.20; α -GLY) (Iftikhar et al., 2019). The α -GLY, which plays an important role in regulating blood glucose levels, is an important enzyme involved in the digestion of carbohydrates (Saleem et al., 2021). α -GLY inhibitors (α -GLYIs) delay the release of D-glucose from carbohydrate-containing diets and the absorption of glucose, thereby lowering plasma glucose levels and suppressing hyperglycemia that can occur at satiety (Ren et al., 2011). As a result of this, α -GLYIs use in DM therapy (Taslami et al., 2018). Although some α -GLYIs, such as acarbose and voglibose (Alomari et al., 2021; Taha et al., 2021), which are widely used clinically to control blood

glucose levels, are effective, they often have side effects such as meteorism and flatulence abdominal distension, and possibly diarrhea (Hollander, 1992; Nakagawa, 2013). In this context, many researchers have turned to the novel drug discovery and development technology and toxicology area to discover alternatives of both ChEs and α -GLY inhibitors (Chen et al., 2013).

Anion transport across cellular membranes is essential for maintaining the normal physiological functions of cells (Poulsen et al., 2010). To date, many small-molecule anion transporters based on urea (Dias et al., 2018), thioureas (Akhtar et al., 2018), sulfonamides (Saha et al., 2016) have been reported (Yu et al., 2019). Moreover, sulfonamide compounds have many biological activities, including anti-Alzheimer's, anticancer, antimicrobial, antiviral, and antidiabetic activities (Figure 1). Thus, sulfonamide compounds derived from urea and its sulfur analogue thiourea have been used continuously to design new bioactive compounds due to their critical pharmacological properties (Akocak et al., 2021; Lolak et al., 2020). In our study, it was synthesized and characterized novel inhibitors with sulfamethazine backbone, which have been important bioactive properties with their chemical structure to discover newly multitarget inhibitors effective on AChE, BChE, and α -GLY. The *in silico* predictions, namely, prediction of ADME and toxicity profiles, molecular docking, and *in vitro* inhibition effects, of the synthesized novel ureido-substituted sulfamethazine derivatives (**2a-f**) were investigated for these enzymes associated with AD and DM.

2. Materials and methods

2.1. Chemistry

Sulfamethazine (SM) (3 mmol) was dissolved in acetonitrile (15–20 mL) and then treated with subsequent isocyanates (3 mmol). The mixture was stirred at room temperature for 3 h and then heated at 50 °C until completion (TLC monitoring). The appeared precipitate was filtered off, washed with diethyl ether (50 mL) as well as water, and dried in vacuo. The obtained pure products (**2a-f**) were characterized in

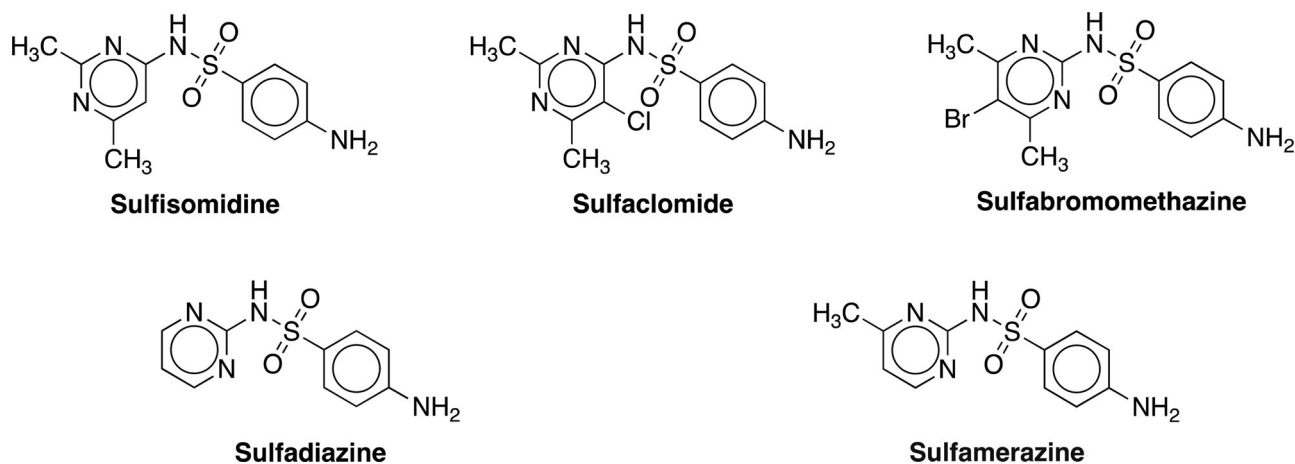
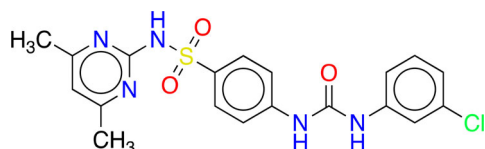


Figure 1. Structure of some commercially available pyrimidinyl sulfonamide derivative drugs.

detail by spectroscopic and analytic methods (FT-IR, $^1\text{H-NMR}$, $^{13}\text{C-NMR}$, elemental analysis, mass analysis, and melting points).

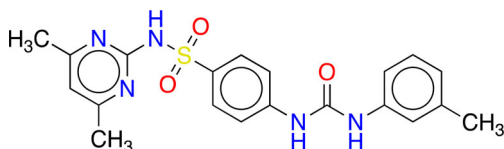
2.2. General procedure for the synthesis of *N*-(4,6-dimethylpyrimidin-2-yl)-4-(3-substitutedphenylureido) benzenesulfonamides (2a-f)

2.2.1. *N*-(4,6-dimethylpyrimidin-2-yl)-4-(3-(3-chlorophenyl)ureido) benzenesulfonamide (2a)



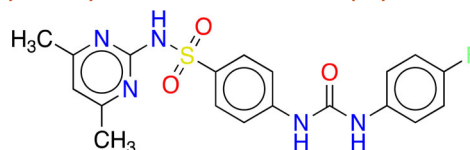
Yield: 75%; Color: white solid; Melting Point: 255–258 °C; Anal. Calcd. for $\text{C}_{19}\text{H}_{18}\text{ClN}_5\text{O}_3\text{S}$ (431.90 g/mol) (%): C, 52.84; H, 4.20; N, 16.22; S, 7.42; Found: C, 52.80; H, 4.18; N, 16.26; S, 7.40; FT-IR (cm^{-1}): 3360, 3329, 3288 (NH), 1707 (C=O), 1625, 1526, 1261, 1134 (symmetric) (S=O), 1079; $^1\text{H-NMR}$ (DMSO- d_6 , 400 MHz, δ ppm): 11.57 (br.s, 1H, -NHSO $_2$), 9.20 (s, 1H, -NH-), 9.03 (s, 1H, -NH-), 7.95 (d, $J = 8.8$ Hz, 2H, Ar-H), 7.73 (s, 1H, Ar-H), 7.63 (d, $J = 8.8$ Hz, 2H, Ar-H), 7.29 (d, $J = 4.4$ Hz, 1H, Ar-H), 7.04 (t, $J = 2.8$ Hz, 1H, Ar-H), 6.70 (s, 1H, Ar-H), 2.24 (s, 6H, -CH $_3$); $^{13}\text{C-NMR}$ (DMSO- d_6 , 100 MHz, δ ppm): 167.83, 156.76, 152.55, 143.85, 141.28, 133.72, 133.56, 130.87, 129.94, 122.33, 118.29, 117.55, 117.34, 114.06, 23.37. $R_f = 0.66$ (methanol/ethylacetate, 2:98); HRMS m/z calculated for $\text{C}_{19}\text{H}_{18}\text{ClN}_5\text{O}_3\text{S}$ $[\text{M} + \text{H}]^+$ 432.0897, found: 432.0880.

2.2.2. *N*-(4,6-dimethylpyrimidin-2-yl)-4-(3-(*m*-tolyl)ureido) benzenesulfonamide (2b)



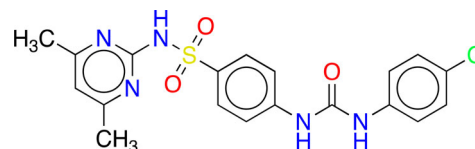
Yield: 62%; Color: white solid; Melting Point: 244–246 °C; Anal. Calcd. for $\text{C}_{20}\text{H}_{21}\text{N}_5\text{O}_3\text{S}$ (411.48 g/mol) (%): C, 58.38; H, 5.14; N, 17.02; S, 7.79; Found: C, 58.35; H, 5.16; N, 17.08; S, 7.76; FT-IR (cm^{-1}): 3362, 3325, 3288 (NH), 1700 (C=O), 1617, 1526, 1262, 1134 (symmetric) (S=O), 1081; $^1\text{H-NMR}$ (DMSO- d_6 , 400 MHz, δ ppm): 11.51 (br.s, 1H, -NHSO $_2$), 9.08 (s, 1H, -NH-), 8.72 (s, 1H, -NH-), 7.93 (d, $J = 8.8$ Hz, 2H, Ar-H), 7.62 (d, $J = 8.4$ Hz, 2H, Ar-H), 7.32 (s, 1H, Ar-H), 7.25–7.13 (m, 2H, Ar-H), 6.80 (d, $J = 7.2$ Hz, 1H, Ar-H), 6.73 (s, 1H, Ar-H), 2.27 (s, 3H, -CH $_3$), 2.25 (s, 6H, -CH $_3$); $^{13}\text{C-NMR}$ (DMSO- d_6 , 100 MHz, δ ppm): 167.86, 156.79, 152.62, 144.37, 139.61, 138.51, 133.24, 129.94, 129.13, 123.48, 119.43, 117.29, 116.09, 114.10, 23.39, 21.64. $R_f = 0.75$ (methanol/ethylacetate, 2:98); HRMS m/z calculated for $\text{C}_{20}\text{H}_{21}\text{N}_5\text{O}_3\text{S}$ $[\text{M} + \text{H}]^+$ 412.1443, found: 412.1447.

2.2.3. *N*-(4,6-dimethylpyrimidin-2-yl)-4-(3-(4-fluorophenyl)ureido) benzenesulfonamide (2c)



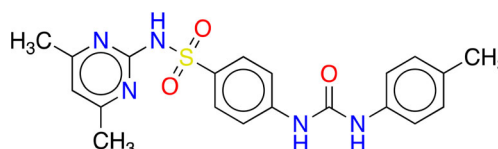
Yield: 78%; Color: white solid; Melting Point: 239–241 °C; Anal. Calcd. for $\text{C}_{19}\text{H}_{18}\text{FN}_5\text{O}_3\text{S}$ (415.44 g/mol) (%): C, 54.93; H, 4.37; N, 16.86; S, 7.72; Found: C, 54.90; H, 4.38; N, 16.87; S, 7.70; FT-IR (cm^{-1}): 3371, 3341, 3231 (NH), 1703 (C=O), 1625, 1508, 1261, 1134 (symmetric) (S=O), 1080; $^1\text{H-NMR}$ (DMSO- d_6 , 400 MHz, δ ppm): 11.55 (br.s, 1H, -NHSO $_2$), 9.11 (s, 1H, -NH-), 8.85 (s, 1H, -NH-), 7.93 (d, $J = 8.8$ Hz, 2H, Ar-H), 7.61 (d, $J = 9.2$ Hz, 2H, Ar-H), 7.49–7.46 (m, 2H, Ar-H), 7.13 (t, 2H, Ar-H), 6.72 (s, 1H, Ar-H), 2.24 (s, 6H, -CH $_3$); $^{13}\text{C-NMR}$ (DMSO- d_6 , 100 MHz, δ ppm): 167.86, 159.24, 156.77, 152.75, 144.12, 136.01, 133.30, 129.93, 120.73, 117.37, 115.70, 114.08, 23.38. $R_f = 0.70$ (methanol/ethylacetate, 2:98); HRMS m/z calculated for $\text{C}_{19}\text{H}_{18}\text{FN}_5\text{O}_3\text{S}$ $[\text{M} + \text{H}]^+$ 416.1193, found: 416.1199.

2.2.4. *N*-(4,6-dimethylpyrimidin-2-yl)-4-(3-(4-chlorophenyl)ureido) benzenesulfonamide (2d)



Yield: 66%; Color: white solid; Melting Point: 237–239 °C; Anal. Calcd. for $\text{C}_{19}\text{H}_{18}\text{ClN}_5\text{O}_3\text{S}$ (431.90 g/mol) (%): C, 52.84; H, 4.20; N, 16.22; S, 7.42; Found: C, 52.82; H, 4.17; N, 16.24; S, 7.41; FT-IR (cm^{-1}): 3352, 3315 (NH), 1717 (C=O), 1621, 1537, 1291, 1140 (symmetric) (S=O), 1097; $^1\text{H-NMR}$ (DMSO- d_6 , 400 MHz, δ ppm): 11.57 (br.s, 1H, -NHSO $_2$), 9.15 (s, 1H, -NH-), 8.96 (s, 1H, -NH-), 7.93 (d, $J = 8.8$ Hz, 2H, Ar-H), 7.61 (d, $J = 8.8$ Hz, 2H, Ar-H), 7.49 (d, $J = 8.8$ Hz, 2H, Ar-H), 7.33 (d, $J = 8.8$ Hz, 2H, Ar-H), 6.73 (s, 1H, Ar-H), 2.24 (s, 6H, -CH $_3$); $^{13}\text{C-NMR}$ (DMSO- d_6 , 100 MHz, δ ppm): 167.83, 156.76, 152.57, 143.96, 138.72, 133.44, 129.93, 129.14, 126.29, 120.45, 117.43, 114.07, 23.39. $R_f = 0.68$ (methanol/ethylacetate, 2:98); HRMS m/z calculated for $\text{C}_{19}\text{H}_{18}\text{ClN}_5\text{O}_3\text{S}$ $[\text{M} + \text{H}]^+$ 432.0897, found: 432.0903.

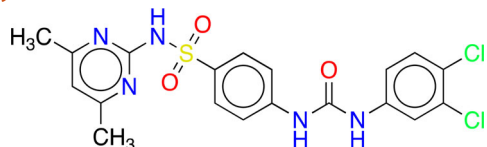
2.2.5. *N*-(4,6-dimethylpyrimidin-2-yl)-4-(3-(*p*-tolyl)ureido) benzenesulfonamide (2e)



Yield: 75%; Color: white solid; Melting Point: 246–249 °C; Anal. Calcd. for $\text{C}_{20}\text{H}_{21}\text{N}_5\text{O}_3\text{S}$ (411.48 g/mol) (%): C, 58.38; H, 5.14; N, 17.02; S, 7.79; Found: C, 58.36; H, 5.17; N, 17.07; S, 7.77; FT-IR (cm^{-1}): 3378, 3354, 3304 (NH), 1707 (C=O), 1631, 1512, 1280, 1139 (symmetric) (S=O), 1084; $^1\text{H-NMR}$

NMR (DMSO- d_6 , 400 MHz, δ ppm): 11.53 (br.s, 1H, $-NHSO_2$), 9.06 (s, 1H, $-NH-$), 8.70 (s, 1H, $-NH-$), 7.91 (d, $J=8.8$ Hz, 2H, Ar-H), 7.60 (d, $J=8.4$ Hz, 2H, Ar-H), 7.34 (d, $J=8.0$ Hz, 2H, Ar-H), 7.09 (d, $J=8.0$ Hz, 2H, Ar-H), 6.74 (s, 1H, Ar-H), 2.25 (s, 6H, $-CH_3$), 2.22 (s, 3H, $-CH_3$); ^{13}C -NMR (DMSO- d_6 , 100 MHz, δ ppm): 167.76, 156.79, 152.67, 144.23, 137.11, 133.12, 131.62, 129.93, 129.69, 119.01, 117.24, 114.11, 23.41, 20.79. $R_f = 0.74$ (methanol/ethylacetate, 2:98); HRMS m/z calculated for $C_{20}H_{21}N_5O_3S$ $[M + H]^+$ 412.1443, found: 412.1423.

2.2.6. *N*-(4,6-dimethylpyrimidin-2-yl)-4-(3-(3,4-dichlorophenyl)ureido) benzenesulfonamide (2f)



Yield: 72%; Color: white solid; Melting Point: 236–239 °C; Anal. Calcd. for $C_{19}H_{17}Cl_2N_5O_3S$ (466.34 g/mol) (%): C, 48.94; H, 3.67; N, 15.02; S, 6.87; Found: C, 48.92; H, 3.63; N, 15.07; S, 6.84; FT-IR (cm^{-1}): 3353, 3289, 3189 (NH), 1707 (C=O), 1629, 1530, 1294, 1133 (symmetric) (S=O), 1081; 1H -NMR (DMSO- d_6 , 400 MHz, δ ppm): 11.54 (br.s, 1H, $-NHSO_2$), 9.22 (s, 1H, $-NH-$), 9.10 (s, 1H, $-NH-$), 7.94 (d, $J=8.4$ Hz, 2H, Ar-H), 7.88 (s, 1H, Ar-H), 7.62 (d, $J=8.4$ Hz, 2H, Ar-H), 7.50 (d, $J=8.8$ Hz, 1H, Ar-H) 7.33 (d, $J=8.8$ Hz, 1H, Ar-H), 6.72 (s, 1H, Ar-H), 2.25 (s, 6H, $-CH_3$); ^{13}C -NMR (DMSO- d_6 , 100 MHz, δ ppm): 167.85, 156.76, 152.49, 143.70, 139.70, 133.76, 131.57, 131.04, 129.90, 124.08, 120.06, 119.06, 117.66, 114.06, 23.37. $R_f = 0.65$ (methanol/ethylacetate, 2:98); HRMS m/z calculated for $C_{19}H_{17}Cl_2N_5O_3S$ $[M + H]^+$ 466.0507, found: 466.0500.

2.3. Biological studies

2.3.1. ChEs and α -GLY inhibition assay

The assays of the AChE and BChE activities were performed by a modified version of the Ellman's method (Ellman et al., 1961), and the inhibitory effect of novel ureido-substituted derivatives with sulfamethazine backbone (**2a-f**) was examined for the AChE (from electric eel; Sigma C2888, Type V-S) and BChE (from equine serum; Sigma C1057) using acetylthiocholine iodide (ATChI; Sigma 01480), and butyrylcholine iodide (BChI; Sigma 20780) as the substrates at pH 8.0 at 37 °C (Atmaca et al., 2019; Mughal et al., 2017). The activity results were monitored spectrophotometrically at 412 nm (Çelik et al., 2020; Gülçin et al., 2016). The α -GLY inhibitory effect of these ureido-substituted sulfamethazine derivatives (**2a-f**) was investigated using p-nitrophenyl-D-glycopyranoside (p-NPG; Sigma N1377) as the substrate at pH 7.4 at 37 °C, as described in previous studies (Topal, 2019a, 2019b). The absorbance values were spectrophotometrically measured at 405 nm (Caglayan, 2019; Güzel et al., 2019).

2.3.2. ChEs and α -GLY kinetic analysis

The inhibition effects of novel ureido-substituted derivatives with sulfamethazine backbone (**2a-f**) were determined with at least five different inhibitor concentrations on AChE, BChE,

and α -GLY. The IC_{50} values of the synthesized agents were calculated from Activity (%)-[Ligand] graphs for each derivative according to our previous studies (Akbaba et al., 2013; Türkeş, 2019b; Türkeş et al., 2015). The inhibition types and K_i constants were found by Lineweaver and Burk's curves as described in previous studies (Demir, 2020; Türkeş et al., 2014, 2016, 2019c). The results were exhibited as mean \pm standard error of the mean (95% confidence intervals). Differences between data sets were considered statistically significant when the p -value was less than 0.05.

2.4. In silico studies

2.4.1. ADME-Tox study

The ADME-Tox profile screening of the novel ureido-substituted inhibitors with sulfamethazine backbone (**2a-f**) pertaining to pre-clinical agent discovery stages was performed using the QikProp module (Durgun et al., 2020) and SwissADME platform (Sever et al., 2020). These ADME-Tox properties include: (i) Molecular weight of the compound; (ii) Computed dipole moment of the compound; (iii) Total solvent-accessible volume in cubic angstroms using a probe with a 1.4 Å Radius; (iv) Octanol/gas partition coefficient; (v) Water/gas partition coefficient; (vi) Octanol/water partition coefficient; (vii) Aqueous solubility; (viii) IC_{50} value for the blockage of HERG K^+ channels; (ix) Apparent Caco-2 cell permeability in nm/sec; (x) Brain/blood partition coefficient; (xi) Apparent MDCK cell permeability in nm/sec; (xii) Skin permeability; (xiii) Prediction of binding to human serum albumin; (xiv) Human oral absorption; (xv) Van der Waals surface area of polar nitrogen and oxygen atoms; (xvi) Number of violations of Lipinski's rule of five (Lipinski et al., 1997); (xvii) Number of violations of Jorgensen's rule of three (Duffy & Jorgensen, 2000); and (xviii) Pan-assay interference compounds alert.

2.4.2. Molecular docking study

The molecular docking analysis, MM-GBSA free binding energy estimations, and design of correlation figures were performed within the Schrödinger Small-Molecule Drug Discovery Suite 2020–3 for Mac (Schrödinger, LLC, NY, USA) using the panels: Maestro (Taslimi et al., 2020b), Protein Preparation Wizard (Türkeş, 2019a), LigPrep (Beydemir et al., 2019), Receptor Grid Generation (Türkeş et al., 2021), and Prime MM-GBSA (Kalaycı et al., 2021). Initially, the crystal structures of AChE (PDB: 4BDT, species *Homo sapiens*) (Mughal et al., 2020), BChE (PDB: 4BDS, species *Homo sapiens*) (Nachon et al., 2013), and α -GLY (PDB: 5NN6, species *Homo sapiens*) (Roig-Zamboni et al., 2017) were downloaded from the Protein Data Bank (Boy et al., 2021; Gündoğdu et al., 2019), prepared and optimized using the Protein Preparation Wizard (Sastry et al., 2013; Türkeş et al., 2019b) integrated into the Maestro software. Afterward, the novel ureido-substituted inhibitors with sulfamethazine backbone (**2a-f**) were built by the ChemDraw (Türkeş et al., 2020) version 19.1 for Mac (PerkinElmer, Inc., Waltham, MA, USA) and suitably optimized for docking by the LigPrep tool (Turhan

et al., 2020; Türkeş et al., 2019a). Epik (Demir et al., 2020; Shelley et al., 2007) with default conditions was used in the OPLS3e force field (Turkan et al., 2019; Türkeş et al., 2020) at pH 7.4 ± 0.5 (Türkeş & Beydemir, 2020). Finally, the grids for 4BDT, 4BDS, and 5NN6 were created using the Receptor Grid Generation tool (Sever et al., 2021), and the Glide extra precision (XP) (Friesner et al., 2006; Türkeş et al., 2020) option of the Ligand Docking tool was utilized to dock the sulfamethazine derivatives (**2a-f**) in the binding site of the enzymes. The docking scores were used to score the poses of these derivatives (**2a-f**) and to evaluate its binding affinity towards the binding site of 4BDT, 4BDS, and 5NN6. Also, MM-GBSA solvation (Işık et al., 2020b) in the VSGB energy model and OPLS3e force field (Işık et al., 2020a) was used to compute the binding energies for the best poses of AChE, BChE, and α -GLY with the novel ureido-substituted inhibitors (**2a-f**) derived from Glide XP docking.

3. Results and discussion

3.1. Drug design strategy and chemistry

The SLC-0111 (PubChem CID: 310360; 4-fluorophenylureido-benzenesulfonamide) was used as a lead molecule for designing *N*-(4,6-dimethylpyrimidin-2-yl)-4-(3-substitutedphenylureido) benzenesulfonamide derivatives (**2a-f**), as this compound recently reached phase II clinical trials for the treatment of advanced metastatic solid tumors (Figure 2) (Lou et al., 2011; Pacchiano et al., 2011). Many different classes of ureido-substituted benzenesulfonamides have been investigated earlier as potent and selective human carbonic anhydrases (*h*CAs) inhibitors (Supuran et al., 1998).

In the present study, we decided to develop ureido-substituted sulfamethazine derivatives as potential AChE, BChE, and α -GLY enzyme inhibitors to see the binding group's

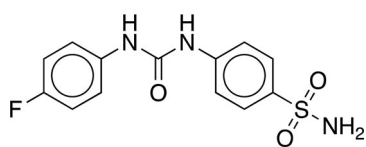
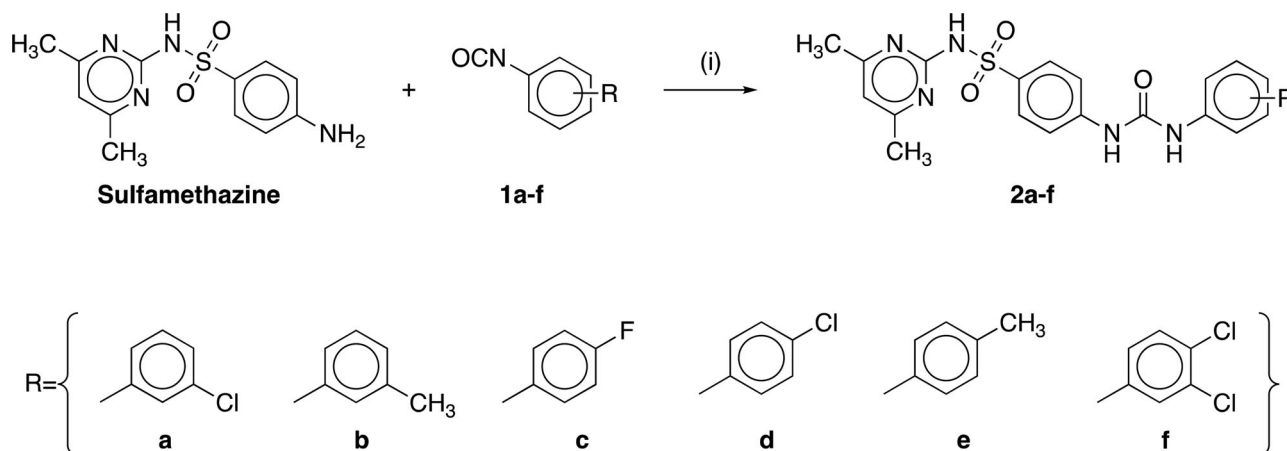


Figure 2. Structure of SCL-0111.



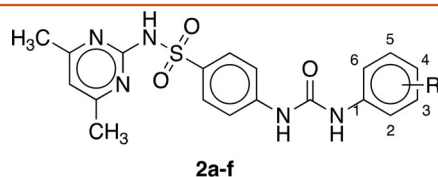
Scheme 1. General synthetic route for the synthesis of the *N*-(4,6-dimethylpyrimidin-2-yl)-4-(3-substitutedphenylureido) benzenesulfonamide derivatives (**2a-f**). Reagent and conditions: (i) MeCN, R.T. for 3 h, then 50 °C for 3–5 h, yields 62–78%.

effect potency. In this study, a series of structurally diverse *N*-(4,6-dimethylpyrimidin-2-yl)-4-(3-substitutedphenylureido) benzenesulfonamides analogs (**2a-f**) were synthesized by a modified procedure presented in previous studies and depicted in Scheme 1 (Pacchiano et al., 2011). Briefly, sulfamethazine was condensed with substituted isocyanates to produce final ureido-substituted sulfamethazine derivatives (**2a-f**). The isocyanates used were: 3-chlorophenyl isocyanate (**1a**), *m*-tolyl isocyanate (**1b**), 4-fluorophenyl isocyanate (**1c**), 4-chlorophenyl isocyanate (**1d**), *p*-tolyl isocyanate (**1e**), and 3,4-dichlorophenyl isocyanate (**1f**) in the series. The chemical structures of the synthesized *N*-(4,6-dimethylpyrimidin-2-yl)-4-(3-substitutedphenylureido) benzenesulfonamides (**2a-f**) were elucidated by using FT-IR, ¹H-NMR, ¹³C-NMR, elemental analysis, mass analysis, and melting point methods. The NMR (¹H-NMR and ¹³C-NMR) spectrums and HR-ESI-MS spectrums of the sulfamethazine derivatives (**2a-f**) are given in Figures S1–S18 (supplementary material).

3.2. Biological study and structure-activity relationship

3.2.1. ChEs and α -GLY inhibition assay

Sulfonamides, which are also called sulfa/sulpha drugs, are synthetic agents containing the sulfonamide chemical group. Sulfa medicines exhibit several activities such as anticonvulsant, anti-bacterial, anti-inflammatory, immunomodulatory, and diuretic effects based on many groups of agents by interfering with cell metabolism. The synthesis of new sulfonamides is carried out to give the compound multi-faceted bioactive properties by adding different groups to known scaffolds. For example, potent some AChE and BChE inhibitors associated with AD that show activity *in vivo* at low concentrations have been developed by synthesizing several sulfonamide analogs (Kosak et al., 2018). In light of these developments, the researchers have focused on the sulfa drug derivatives synthesized as versatile agents against metabolic diseases in recent years, and many sulfonamide derivatives are improved for the treatment of AD and other central nervous system disorders, various cancer kinds, psychosis, diabetes, and many more complex diseases (Apaydın & Török, 2019; Khanfar et al., 2013). The increase in AChE and BChE activities that hydrolyzes the

Table 1. The inhibition results of novel ureido-substituted inhibitors with sulfamethazine backbone (**2a-f**) against AChE, BChE, and α -GLY enzymes.

Compound ID	R	IC_{50} (nM)				K_i (nM)				
		AChE	R^2	BChE	R^2	AChE	BChE	α -GLY		
2a	3-Cl	176.32	0.9733	145.05	0.9904	9.05	0.9482	136.07 \pm 25.01	124.02 \pm 10.44	12.80 \pm 3.05
2b	3-CH ₃	244.38	0.9394	203.05	0.9732	68.76	0.9437	204.95 \pm 11.47	147.04 \pm 27.06	79.22 \pm 14.66
2c	4-F	81.27	0.9720	49.05	0.9881	24.10	0.9487	56.07 \pm 9.53	38.05 \pm 7.04	32.05 \pm 4.85
2d	4-Cl	143.98	0.9913	184.23	0.9557	22.03	0.9594	125.04 \pm 10.25	145.26 \pm 20.48	27.65 \pm 5.98
2e	4-CH ₃	198.37	0.9882	154.26	0.9673	58.34	0.9382	135.86 \pm 14.72	126.74 \pm 26.51	65.06 \pm 7.05
2f	3,4-diCl	72.85	0.9588	65.23	0.9127	18.34	0.9903	64.68 \pm 7.08	54.07 \pm 9.04	29.92 \pm 3.67
THA ^a	–	145.31	0.9734	208.03	0.9881	–	–	112.05 \pm 24.05	177.15 \pm 39.05	–
ACR ^b	–	–	–	–	–	36.58	0.9420	–	–	40.37 \pm 3.16

^aTacrine.^bAcarbose.

neurotransmitter ACh causes neurodegenerative diseases such as AD by increasing amyloid protein formation. Strong inhibition of ChEs is an important option to consider when treating the disease to reduce the hydrolysis of this neurotransmitter and accepted as an approach in the treatment of AD (Rao et al., 2007). It may be possible to balance the blood glucose level to a normal level by inhibiting the α -GLY in DM disease, which is known to be associated with AD. It has also been reported that α -GLYs besides their antidiabetic properties have the potential to treat a variety of diseases, including hepatitis, cancer, and heart conditions (Fischer et al., 1996; McCulloch et al., 1983). In this study, it was set out to investigate the influences of the new inhibitors with sulfamethazine backbone (**2a-f**) as multi-target cholinesterase and α -glucosidase inhibitors on AChE, BChE, and α -GLY. All the analogues were analyzed for their inhibitory activities versus metabolic enzymes as AChE, BChE, and α -GLY, in comparison with the clinically used medicines tacrine (THA) and acarbose (ACR). The inhibition data (IC_{50} and K_i values) for all novel ureido-substituted inhibitors with sulfamethazine backbone (**2a-f**) are summarized in Table 1.

AChE was inhibited by all derivatives (**2a-f**) with a variety of potencies. All novel ureido-substituted inhibitors with sulfamethazine backbone (**2a-f**) were potent AChE inhibitors with IC_{50} s in the range of 72.85–244.38 nM, and K_i s ranging between 56.07 \pm 9.53 nM and 204.95 \pm 11.47 nM. The most active analogues in this series (**2a-f**) were 4-fluoro substituted derivative **2c** and, 3,4-dichloro substituted derivative **2f** with K_i s of 56.07 \pm 9.53 nM, and 64.68 \pm 7.08 nM, respectively, compared to standard inhibitor THA (K_i of 112.05 \pm 24.05 nM). The order of inhibitory activities for the novel ureido-substituted derivatives with sulfamethazine backbone (**2a-f**) versus AChE decreased in the order of **2c** (4-fluoro substituted) > **2f** (3,4-dichloro substituted) > **2d** (4-chloro substituted) > **2e** (4-methyl substituted) > **2a** (3-chloro substituted) > **2b** (3-methyl substituted).

BChE, one of the other cholinesterases, was inhibited by the novel ureido-substituted inhibitors with sulfamethazine backbone (**2a-f**) in nanomolar levels with IC_{50} s ranging from

49.05 to 203.05 nM, and K_i s in the range of 38.05 \pm 7.04–147.04 \pm 27.06 nM. Moreover, all derivatives (**2a-f**) showed more potent inhibitory effects on BChE as compared to THA (K_i of 177.15 \pm 39.05 nM). Analogue **2c** bearing the fluoro moiety at the 4th position was the most potent inhibitor of BChE with a K_i of 38.05 \pm 7.04 nM, and the second most potent inhibitor was 3,4-dichloro substituted sulfamethazine derivative **2f** with a K_i of 54.07 \pm 9.04 nM. The BChE inhibitory activities for the novel ureido-substituted compounds with sulfamethazine backbone (**2a-f**) reduced in the order of **2c** (4-fluoro substituted) > **2f** (3,4-dichloro substituted) > **2a** (3-chloro substituted) > **2e** (4-methyl substituted) > **2d** (4-chloro substituted) > **2b** (3-methyl substituted). On the other hand, fluoro substitution at the 4th position and 3,4-dichloro substitution made better ChEs inhibitors as compared to other analogues that have been studied in the current work. Moreover, 4-fluoro substituted derivative **2c** (K_i s for AChE and BChE 56.07 \pm 9.53 nM and 38.05 \pm 7.04 nM, respectively) was identified as the most potent AChE inhibitor in this series (**2a-f**).

All the synthesized the novel ureido-substituted inhibitors with sulfamethazine backbone (**2a-f**) exhibited activity in nanomolar levels as α -GLY inhibitors with the IC_{50} and K_i values in the range of 9.05–68.76 nM, and 12.80 \pm 3.05–79.22 \pm 14.66 nM, respectively. Accordingly, these analogues (except compounds **2b** and **2e**) were determined to be more effective inhibitors, compared to ACR as a standard agent with a K_i value of 40.37 \pm 3.16 nM. The results revealed that derivatives with chloro moiety at the 3, and 4th position played a crucial role in α -GLY inhibitory activity. In particular, the most active compounds in this series were 3-chloro substituted compound **2a**, 4-chloro substituted analogue **2d**, and 3,4-dichloro substituted derivative **2f** with K_i s of 12.80 \pm 3.05 nM, 27.65 \pm 5.98 nM, and 29.92 \pm 3.67 nM, respectively. In this respect, it was found that the inhibitory potency order of the novel ureido-substituted analogues with sulfamethazine backbone (**2a-f**) was **2a** (3-chloro substituted) > **2d** (4-chloro substituted) > **2f** (3,4-dichloro

substituted) > **2c** (4-fluoro substituted) > **2e** (4-methyl substituted) > **2b** (3-methyl substituted).

On the other hand, it showed that the methyl substitution on para- and meta-position dramatically lower the AChE, BChE, and α -GLY activity, as it can be seen in the compounds **2b** and **2e**. These cases may be useful strategies to develop ChEs and α -GLY inhibitory activity. It was also determined from *in silico* studies that the presence of these fragments increases the activity. In this direction, many studies have indicated that ureido-substituted sulfamethazine derivatives exhibit significant metabolic enzyme inhibition. In this context, the study by Akocak et al. (2021) reported that a series of six *N*-carbamimidoyl-4-(3-substitutedphenylureido) benzenesulfonamide derivatives (**2a-f**) were synthesized, and their inhibition activities investigated for α -GLY, AChE, and BChE by spectrophotometric methods. They found that novel derivatives with sulfaguanidine backbone (**2a-f**) exhibited effective inhibitory profiles with IC_{50} s in the range of 94.38–409.13 nM, and K_i s ranging between 103.94 and 491.55 nM against α -GLY, with IC_{50} s ranging between 523.05 and 1094.23 nM, K_i s in the range of 481.04–913.43 nM versus AChE, and with IC_{50} s in the range of 660.40–1058.03 nM, and K_i s ranging from 598.47 to 904.73 nM against BChE. Işık et al. (2020c) reported that investigated the effects of some sulfonamide derivatives (**S1-S4** and **S1i-S4i**) on AChE. They found that the synthesized 4-aminobenzenesulfonamides had potential inhibitor properties with different inhibition types for AChE with K_i constants in the range of 2.54 ± 0.22 – 299.60 ± 8.73 μ M. Taslimi et al. (2020a) synthesized that the derivatives of amine (**1i-11i**) and imine sulfonamides (**1-11**) and investigated the effects of the synthesized derivatives on AChE, α -GLY, and glutathione S-transferase (GST) enzymes. K_i values of the series for AChE, α -GLY, and GST were found in the range of 2.26 ± 0.45 – 82.46 ± 14.74 μ M, 95.73 ± 13.67 – 1154.65 ± 243.66 μ M, and 22.76 ± 1.23 – 49.29 ± 4.49 μ M, respectively.

In a study, Gokcen et al. (2016) reported that four groups of sulfonamide derivatives, having isoxazole, pyridine, pyrimidine, thiazole, and thiadiazole groups, synthesized, and their inhibition activities against *hCA* I and II isoenzymes evaluated. They determined that novel derivatives with sulfamethazine backbone (**5c-8c**) demonstrated activity in nanomolar levels as *hCA* I, and *hCA* II inhibitors with IC_{50} values in the range of 9.07–27.72 nM, and 8.77 to 49.51 nM and K_i constants in the range of 7.01–27.18 nM, and 5.74–137.96 nM, respectively. In another study, Hamad et al. (2020) reported that a new series of Schiff base derivatives of (*E*)-4-(benzylideneamino)-*N*-(4,6-dimethylpyr-imidin-2-yl)benzenesulfonamide (**3a-3f**) were synthesized. Synthesized compounds were evaluated for their Jack Bean urease inhibitory activity. It was determined that all derivatives (**3a-3f**) showed potent inhibitory activity, ranging between IC_{50} s 3.78 ± 3.23 μ M and 12.90 ± 2.84 μ M, as compared to standard thiourea (IC_{50} of 20.03 ± 2.03 μ M). Furthermore, to evaluate the drug-likeness of derivatives, ADME prediction was made, and all analogues (**3a-3f**) were determined to be non-toxic and have passive gastrointestinal absorption. In another study, Tugrak et al. (2020) synthesized the novel compounds

with the chemical structure of *N*-({4-[*N'*-(substituted)sulfamoyl]phenyl}carbamoithioly)benzamide (**1a-g**) and 4-fluoro-*N*-({4-[*N'*-(substituted)sulfamoyl]phenyl}carbamoithioly)benzamide (**2a-g**) potent and selective *hCA* I and II isoenzymes inhibitors. The aryl part of compounds **1g** and **2g** from the derivatives in the series was sulfamethazine. The K_i constants of derivative **1g** were 59.55 ± 13.07 nM (*hCA* I) and 12.19 ± 2.24 nM (*hCA* II), whereas the K_i constants of analogue **2g** were 55.95 ± 10.72 nM (*hCA* I) and 47.96 ± 7.91 nM (*hCA* II). Comparing the K_i values of acetazolamide (82.13 ± 4.56 nM for *hCA* I and 50.27 ± 3.75 nM for *hCA* II), with compounds **1g** and **2g** demonstrated promising and selective inhibitory effects against the *hCA* I and II isoenzymes, the main target proteins.

3.3. In silico studies

3.3.1. ADME-Tox study

ADME-Tox-related parameters were determined for novel ureido-substituted inhibitors with sulfamethazine backbone (**2a-f**), and the results are summarized in Table 2. Also, diagrams showing 'drug-likeness' descriptors for **2a** and **2c**, which are the most active derivatives in this series, are given in Figure 3. None of six ureido-substituted sulfamethazine derivatives (**2a-f**) were found to have no Lipinski's rule violation, and only two derivatives showed one Jorgensen's rule violation. According to Lipinski's rule, the octanol/water partition coefficient (QPlogPo/w) value should be ≤ 5 . For these analogues (**2a-f**) bearing 3-chlorophenyl, *m*-tolyl, 4-fluorophenyl, 4-chlorophenyl, *p*-tolyl, and 3,4-dichlorophenyl moiety QPlogPo/w values ranging from 2.10 to 2.72. The predicted number of hydrogen bonds donated (donorHB ≤ 5) and the predicted number of hydrogen bonds accepted (accptHB ≤ 10) for all the derivatives (**2a-f**) were in agreement with the drug-likeness requirements of Lipinski's rule of five. Molecular weight (MW) is a crucial factor for binding at the active site. It was found that all compounds (**2a-f**) have MW between 411.48 and 466.34 (the reference value of MW is < 500 on the report of Lipinski's). The aqueous solubility (QPlogS) of a compound importantly affects its distribution and absorption characteristics. Usually, a high solubility goes along with good absorption. Considering Jorgensen's rule, the QPlogS value should be ≤ -5.7 . Only compound **2d** (QPlogS: -5.79) and compound **2f** (QPlogS: -6.07) presented solubility values out of the limits. This is why these two compounds (**2d** and **2f**) displayed one violation of Jorgensen's rule. The predicted apparent Caco-2 cell permeability (QPpCaco values in the range of 156.85–214.39) of the analyzed derivatives (**2a-f**) indicated excellent results (QPpCaco value should be >22 nm/s) and agreed with Jorgensen's rule of three. To sum up, computed ADME-Tox properties confirmed novel ureido-substituted inhibitors with sulfamethazine backbone (**2a-f**) as hit-agents displaying suitable drug-like properties.

Table 2. ADME-Tox related parameters of novel ureido-substituted inhibitors with sulfamethazine backbone (**2a-f**).

Principal descriptors	2a	2b	2c	2d	2e	2f	Standard range
MW ^a	431.90	411.48	415.44	431.90	411.48	466.34	130.0–725.0
Dipole ^b	11.42	8.46	7.94	7.83	7.77	8.80	1.0–12.5
Volume ^c	1277.79	1288.65	1261.35	1289.46	1305.05	1317.66	500.0–2000.0
QPlogPoct ^d	25.72	24.80	24.67	25.09	24.89	25.77	8.0–35.0
QPlogPw ^e	18.01	17.88	18.09	18.07	18.01	17.78	4.0–45.0
QPlogPo/w ^f	2.31	2.10	2.23	2.48	2.29	2.72	–2.0–6.5
QPlogS ^g	–5.46	–5.21	–5.43	–5.79	–5.61	–6.07	–6.5–0.5
QPlogHERG ^h	–5.46	–5.39	–5.78	–5.81	–5.80	–5.37	concern below –5
QPPCaco ⁱ	156.85	167.90	214.39	214.34	213.96	159.93	<25 poor–great > 500
QPlogBB ^j	–1.52	–1.66	–1.48	–1.44	–1.63	–1.40	–3.0–1.2
QPPMDCK ^k	245.49	105.09	244.75	334.14	135.72	518.83	<25 poor. great > 500
QPlogKp ^l	–3.09	–3.08	–2.73	–2.79	–2.79	–3.22	–8.0–1.0
QPlogKhsa ^m	–0.17	–0.15	–0.23	–0.16	–0.13	–0.81	–1.5–1.5
HOA ⁿ	79.74	79.07	81.70	83.16	82.03	82.34	<25% poor–high > 80%
PSA ^o	116.47	115.66	116.91	116.89	116.70	116.10	7.0–200.0
Rule of five ^p	0	0	0	0	0	0	max. 4
Rule of three ^q	0	0	0	1	0	1	max. 3
PAINS ^r	0	0	0	0	0	0	–

^aThe molecular weight of the compound.

^bComputed dipole moment of the compound.

^cTotal solvent-accessible volume in cubic angstroms using a probe with a 1.4 Å Radius.

^dOctanol/gas partition coefficient.

^eWater/gas partition coefficient.

^fOctanol/water partition coefficient.

^gAqueous solubility.

^hIC₅₀ value for the blockage of HERG K⁺ channels.

ⁱApparent Caco-2 cell permeability in nm/sec.

^jBrain/blood partition coefficient.

^kApparent MDCK cell permeability in nm/sec.

^lSkin permeability.

^mPrediction of binding to human serum albumin.

ⁿHuman oral absorption.

^oVan der Waals surface area of polar nitrogen and oxygen atoms.

^pNumber of violations of Lipinski's rule of five.

^qNumber of violations of Jorgensen's rule of three.

^rPan-assay interference compounds alert.



Figure 3. Diagrams showing 'drug-likeness' descriptors for compound **2a** (*N*-(4,6-dimethylpyrimidin-2-yl)-4-(3-(3-chlorophenyl)ureido) benzenesulfonamide) (left) and compound **2c** (*N*-(4,6-dimethylpyrimidin-2-yl)-4-(3-(4-fluorophenyl)ureido) benzenesulfonamide) (right) from novel ureido-substituted inhibitors with sulfamethazine backbone. The colored zone is a suitable physicochemical space for oral bioavailability. LIPO, lipophilicity; SIZE, molecular weight; POLAR, polarity; INSOLU, insolubility; INSATU, insaturation; FLEX, flexibility.

3.3.2. Molecular docking study

To better understand the interaction of the novel ureido-substituted inhibitors with sulfamethazine backbone (**2a-f**) with 4BDT, 4DBS, and 5NN6, the most potent AChE, BChE, and α -GLY inhibitors **2c** (for ChEs) and **2a** (for α -GLY) were docked in the binding sites of these enzymes. For the redocking computes, the structures of crystal ligands including, HUW (Huprine W, PubChem Ref.: 71463576), THA (Tacrine, PubChem Ref.: 1935), and MIG ((2*R*,3*R*,4*R*,5*S*)-1-(2-

hydroxyethyl)-2-(hydroxymethyl)piperidine-3,4,5-triol, PubChem Ref.: 441314) in the active sites were used (Figure 4). The docked poses of HUW and THA overlapped with the poses in the X-ray crystal structure (PDBs: 4BDT, and 4BDS) at a root mean square deviation (RMSD) values of 0.08 and 0.06 Å, respectively, whereas the docked pose of MIG and X-ray structure (PDB: 5NN6) displayed an RMSD value of 0.80 Å. After that, in the present docking study, the docking patterns of HUW, THA, and MIG were compared with that of

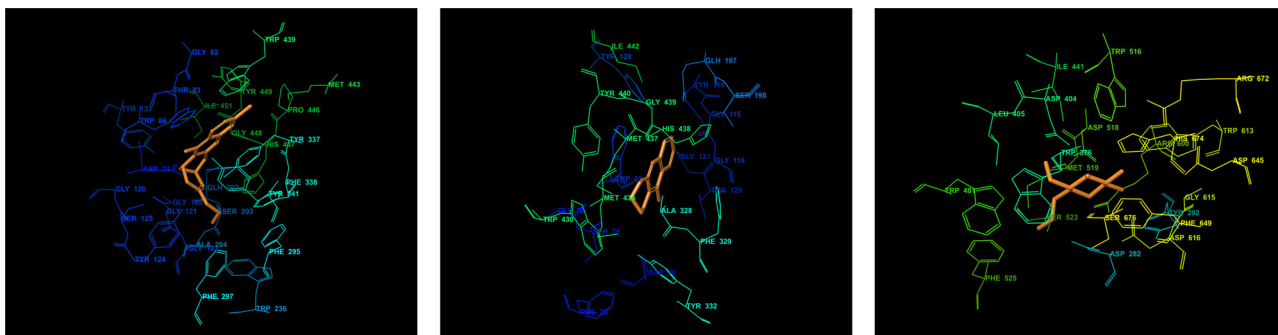


Figure 4. The binding sites of AChE (PDB: 4BDT) (left), BChE (PDB: 4BDS) (middle), and α -GLY (PDB: 5NN6) (right) with the docked poses of the native ligands HUW ($C_{18}H_{19}ClN_2O$: Huprine W, PubChem Ref.: 71463576), THA ($C_{13}H_{14}N_2$: Tacrine, PubChem Ref.: 1935), and MIG ($C_8H_{17}NO_5$: (2*R*,3*R*,4*R*,5*S*)-1-(2-hydroxyethyl)-2-(hydroxymethyl)piperidine-3,4,5-triol, PubChem Ref.: 441314), respectively.

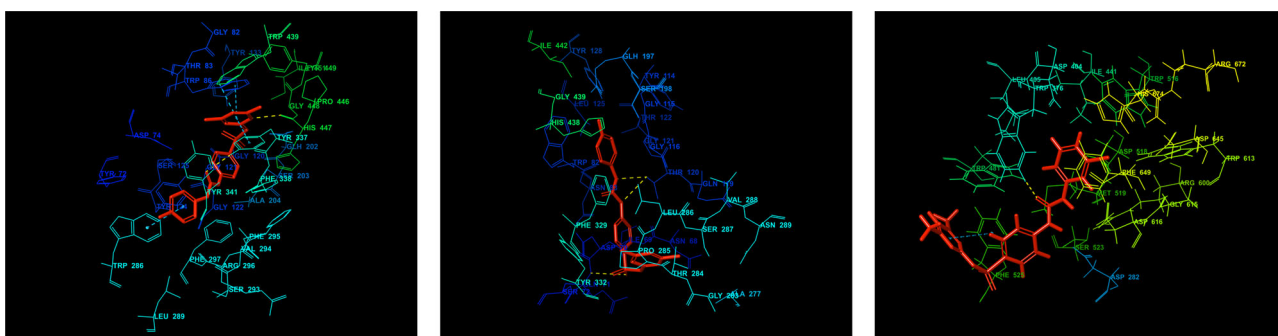


Figure 5. The three-dimensional binding modes of novel ureido-substituted inhibitors **2c** (*N*-(4,6-dimethylpyrimidin-2-yl)-4-(3-(4-fluorophenyl)ureido) benzenesulfonamide) and **2a** (*N*-(4,6-dimethylpyrimidin-2-yl)-4-(3-(3-chlorophenyl)ureido) with sulfamethazine backbone in the binding sites of AChE (4BDT with compound **2c**) (left), BChE (4BDS with compound **2c**) (middle), and α -GLY (5NN6 with compound **2a**) (right).

compound **2c** for AChE and BChE (K_i s: 56.07 ± 9.53 nM and 38.05 ± 7.04 nM, respectively) and compound **2a** for α -GLY (K_i : 12.80 ± 3.05 nM), the most potent compounds in this series (**2a-f**). The binding interactions of the inhibitors with AChE, BChE, and α -GLY are displayed in Figure 5.

A docking score of -8.01 kcal/mol and MM-GBSA value of -29.27 kcal/mol indicated that compound **2c** is a tight binder for AChE. The carboxyl moiety and pyrimidine nitrogen atom formed hydrogen-bonding with residues Tyr337 (distance 1.88 Å) and His447 (distance 1.75 Å), respectively, while benzene and pyrimidine rings displayed $\pi - \pi$ interaction with Trp86, Trp286, and Tyr337. However, derivative **2c** displayed that residues Tyr72, Asp74, Thr83, Tyr124, Gly120, Gly121, Gly122, Glh202, Ser203, Phe295, Arg296, Phe297, Phe338, Tyr341, Trp439, Pro446, Gly448, and Tyr449 play significant roles in the binding of the ligand with AChE. The docking showed that derivative **2c** (docking score of -5.31 kcal/mol and MM-GBSA value of -25.78 kcal/mol) formed three H-bond interactions with residues Gln71 (distance 2.80 Å) and Thr120 (distances 1.94 and 2.60 Å) of BChE. Nevertheless, hydrophobic interactions were monitored between compound **2c** and residues Ile69, Trp82, Tyr114, Leu125, Tyr128, Pro285, Leu286, Phe329, and Tyr332. Structurally, there was a relative correlation between the number of H-bonds and the MM-GBSA value. Accordingly, compound **2a** (docking score of -3.43 kcal/mol and MM-GBSA value of 10.58 kcal/mol) has an H-bond with Trp481

(distance 2.16 Å). It acted also $\pi - \pi$ interaction with Phe525 from the binding site residues of α -GLY. Moreover, the derivative **2a** has that hydrophobic fragments, namely, Trp376, Leu405, Ile441, Trp481, Trp516, Met519, Phe525, Trp613, and Phe649.

4. Conclusion

In conclusion, a series of novel ureido-substituted derivatives with sulfamethazine backbone (**2a-f**) were synthesized and characterized in detail by spectroscopic and analytic methods. *N*-(4,6-dimethylpyrimidin-2-yl)-4-(3-substitutedphenylureido) benzenesulfonamide derivatives (**2a-f**) were first assayed to inhibit AChE, BChE, and α -GLY. The inhibitory activity was more intense versus ChEs compared to standard inhibitors THA and ACR, which, in turn, displayed an inhibition stronger with respect to α -GLY. The effect of derivatives on the enzymes varied according to their molecular structures and positions. Potent novel ureido-substituted derivatives with sulfamethazine backbone (**2a-f**) were detected towards ChEs with a high interest towards the AChE. A derivative was identified, namely the 4-fluorophenylureido **2c**, which displayed a strong inhibitory action versus AChE and BChE. Additionally, an exhaustive *in silico* ligand/enzyme interaction research was performed with the three metabolic enzymes by Glide XP, MM-GBSA, and ADME-Tox predicts.

Disclosure statement

No potential conflict of interest was reported by the authors.

Funding

This work was supported by the Research Fund of Anadolu University (grant number 16105681).

ORCID

Cüneyt Türkeş  <http://orcid.org/0000-0002-2932-2789>
Parham Taslimi  <http://orcid.org/0000-0002-3171-0633>
Mustafa Durgun  <http://orcid.org/0000-0003-3012-7582>
İlhami Gülçin  <http://orcid.org/0000-0001-5993-1668>

References

- Abbott, C., Mackness, M., Kumar, S., Olukoga, A., Gordon, C., Arrol, S., Bhatnagar, D., Boulton, A., & Durrington, P. (1993). Relationship between serum butyrylcholinesterase activity, hypertriglyceridaemia and insulin sensitivity in diabetes mellitus. *Clinical Science*, *85*(1), 77–81. <https://doi.org/10.1042/cs0850077>.
- Akbaba, Y., Türkeş, C., Polat, L., Söyüt, H., Şahin, E., Menzek, A., Göksu, S., & Beydemir, Ş. (2013). Synthesis and paroxonase activities of novel bromophenols. *Journal of Enzyme Inhibition and Medicinal Chemistry*, *28*(5), 1073–1079. <https://doi.org/10.3109/14756366.2012.715287>.
- Akhtar, N., Saha, A., Kumar, V., Pradhan, N., Panda, S., Morla, S., Kumar, S., & Manna, D. (2018). Diphenylethylenediamine-based potent anionophores: Transmembrane chloride ion transport and apoptosis inducing activities. *ACS Applied Materials & Interfaces*, *10*(40), 33803–33813. <https://doi.org/10.1021/acsami.8b06664>.
- Akokcak, S., Taslimi, P., Lolak, N., Işık, M., Durgun, M., Budak, Y., Türkeş, C., Gülçin, İ., & Beydemir, Ş. (2021). Synthesis, characterization, and inhibition study of novel substituted phenylureido sulfaguanidine derivatives as α -glycosidase and cholinesterase inhibitors. *Chemistry & Biodiversity*, *18*(4), e2000958. <https://doi.org/10.1002/cbdv.202000958>.
- Alomari, M., Taha, M., Rahim, F., Selvaraj, M., Iqbal, N., Chigurupati, S., Hussain, S., Uddin, N., Almandil, N. B., & Nawaz, M. (2021). Synthesis of indole-based-thiadiazole derivatives as a potent inhibitor of α -glucosidase enzyme along with in silico study. *Bioorganic Chemistry*, *108*, 104638. <https://doi.org/10.1016/j.bioorg.2021.104638>.
- Apaydın, S., & Török, M. (2019). Sulfonamide derivatives as multi-target agents for complex diseases. *Bioorganic & Medicinal Chemistry Letters*, *29*(16), 2042–2050. <https://doi.org/10.1016/j.bmcl.2019.06.041>.
- Atmaca, U., Daryadel, S., Taslimi, P., Çelik, M., & Gülçin, İ. (2019). Synthesis of β -amino acid derivatives and their inhibitory profiles against some metabolic enzymes. *Archiv Der Pharmazie*, *352*(12), 1900200. <https://doi.org/10.1002/ardp.201900200>.
- Benham, C., Bolton, T., & Lang, R. (1985). Acetylcholine activates an inward current in single mammalian smooth muscle cells. *Nature*, *316*(6026), 345–347. <https://doi.org/10.1038/316345a0>.
- Beydemir, Ş., Türkeş, C., & Yalçın, A. (2019). Gadolinium-based contrast agents: In vitro paraoxonase 1 inhibition, in silico studies. *Drug and Chemical Toxicology*, *1*–10. <https://doi.org/10.1080/01480545.2019.1620266>.
- Boy, S., Türkan, F., Beytur, M., Aras, A., Akyıldırım, O., Karaman, H. S., & Yüksek, H. (2021). Synthesis, design, and assessment of novel morpholine-derived Mannich bases as multifunctional agents for the potential enzyme inhibitory properties including docking study. *Bioorganic Chemistry*, *107*, 104524. <https://doi.org/10.1016/j.bioorg.2020.104524>.
- Caglayan, C. (2019). The effects of naringin on different cyclophosphamide-induced organ toxicities in rats: Investigation of changes in some metabolic enzyme activities. *Environmental Science and Pollution Research*, *26*(26), 26664–26673. <https://doi.org/10.1007/s11356-019-05915-3>.
- Çelik, H., Kandemir, F. M., Caglayan, C., Özdemir, S., Çomaklı, S., Kucukler, S., & Yardım, A. (2020). Neuroprotective effect of rutin against colistin-induced oxidative stress, inflammation and apoptosis in rat brain associated with the CREB/BDNF expressions. *Molecular Biology Reports*, *47*(3), 2023–2034. <https://doi.org/10.1007/s11033-020-05302-z>.
- Chen, Y.-G., Li, P., Li, P., Yan, R., Zhang, X.-Q., Wang, Y., Zhang, X.-T., Ye, W.-C., & Zhang, Q.-W. (2013). α -Glucosidase inhibitory effect and simultaneous quantification of three major flavonoid glycosides in *Microctis folium*. *Molecules*, *18*(4), 4221–4232. <https://doi.org/10.3390/molecules18044221>.
- Chuiko, G. (2000). Comparative study of acetylcholinesterase and butyrylcholinesterase in brain and serum of several freshwater fish: Specific activities and in vitro inhibition by DDVP, an organophosphorus pesticide. *Comparative Biochemistry and Physiology Part C*, *127*(3), 233–242. [https://doi.org/10.1016/S0742-8413\(00\)00150-X](https://doi.org/10.1016/S0742-8413(00)00150-X).
- Collins, A. L., Aitken, T. J., Greenfield, V. Y., Ostlund, S. B., & Wassum, K. M. (2016). Nucleus accumbens acetylcholine receptors modulate dopamine and motivation. *Neuropsychopharmacology*, *41*(12), 2830–2838. <https://doi.org/10.1038/npp.2016.81>.
- Demir, Y. (2020). Naphthoquinones, benzoquinones, and anthraquinones: Molecular docking, ADME and inhibition studies on human serum paraoxonase-1 associated with cardiovascular diseases. *Drug Development Research*, *81*(5), 628–636. <https://doi.org/10.1002/ddr.21667>.
- Demir, Y., Türkeş, C., & Beydemir, Ş. (2020). Molecular docking studies and inhibition properties of some antineoplastic agents against paraoxonase-I. *Anti-Cancer Agents in Medicinal Chemistry*, *20*(7), 887–896. <https://doi.org/10.2174/1871520620666200218110645>.
- Dias, C. M., Li, H., Valkenier, H., Karagiannidis, L. E., Gale, P. A., Sheppard, D. N., & Davis, A. P. (2018). Anion transport by ortho-phenylene bis-ureas across cell and vesicle membranes. *Organic & Biomolecular Chemistry*, *16*(7), 1083–1087. <https://doi.org/10.1039/C7OB02787G>.
- Duffy, E. M., & Jorgensen, W. L. (2000). Prediction of properties from simulations: Free energies of solvation in hexadecane, octanol, and water. *Journal of the American Chemical Society*, *122*(12), 2878–2888. <https://doi.org/10.1021/ja993663t>.
- Durgun, M., Türkeş, C., Işık, M., Demir, Y., Saklı, A., Kuru, A., Güzel, A., Beydemir, Ş., Akocak, S., & Osman, S. M. (2020). Synthesis, characterisation, biological evaluation and in silico studies of sulphonamide Schiff bases. *Journal of Enzyme Inhibition and Medicinal Chemistry*, *35*(1), 950–962. <https://doi.org/10.1080/14756366.2020.1746784>.
- Ellman, G. L., Courtney, K. D., Andres, V., Jr., & Featherstone, R. M. (1961). A new and rapid colorimetric determination of acetylcholinesterase activity. *Biochemical Pharmacology*, *7*(2), 88–95. [https://doi.org/10.1016/0006-2952\(61\)90145-9](https://doi.org/10.1016/0006-2952(61)90145-9).
- Fischer, P., Karlsson, G., Butters, T., Dwek, R., & Platt, F. (1996). N-butyl-deoxyjirimycin-inhibition of human immunodeficiency virus entry correlates with changes in antibody recognition of the V1/V2 region of gp120. *Journal of Virology*, *70*(10), 7143–7152.
- Francis, P. T. (2005). The interplay of neurotransmitters in Alzheimer's disease. *CNS Spectrums*, *10*(S18), 6–9. <https://doi.org/10.1017/s1092852900014164>.
- Friesner, R. A., Murphy, R. B., Repasky, M. P., Frye, L. L., Greenwood, J. R., Halgren, T. A., Sanschagrin, P. C., & Mainz, D. T. (2006). Extra precision glide: Docking and scoring incorporating a model of hydrophobic enclosure for protein – ligand complexes. *Journal of Medicinal Chemistry*, *49*(21), 6177–6196. <https://doi.org/10.1021/jm051256o>.
- Gokcen, T., Gulcin, I., Ozturk, T., & Goren, A. C. (2016). A class of sulfonamides as carbonic anhydrase I and II inhibitors. *Journal of Enzyme Inhibition and Medicinal Chemistry*, *31*(suppl 2), 180–188. <https://doi.org/10.1080/14756366.2016.1198900>.
- Gülçin, İ., Scozzafava, A., Supuran, C. T., Koksall, Z., Turkan, F., Çetinkaya, S., Bingöl, Z., Huyut, Z., & Alwasel, S. H. (2016). Rosmarinic acid inhibits some metabolic enzymes including glutathione S-transferase, lactoperoxidase, acetylcholinesterase, butyrylcholinesterase and carbonic anhydrase isoenzymes. *Journal of Enzyme Inhibition and Medicinal Chemistry*, *31*(6), 1698–1702. <https://doi.org/10.3109/14756366.2015.1135914>.

- Gündođdu, S., Türkeş, C., Arslan, M., Demir, Y., & Beydemir, Ş. (2019). New Isoindole-1, 3-dione substituted sulfonamides as potent inhibitors of carbonic anhydrase and acetylcholinesterase: Design, synthesis, and biological evaluation. *ChemistrySelect*, 4(45), 13347–13355. <https://doi.org/10.1002/slct.201903458>.
- Güzel, E., Koçyiğit, Ü. M., Arslan, B. S., Ataş, M., Taslimi, P., Gökalp, F., Nebiođlu, M., Şişman, İ., & Gulçin, İ. (2019). Aminopyrazole-substituted metallophthalocyanines: Preparation, aggregation behavior, and investigation of metabolic enzymes inhibition properties. *Archiv Der Pharmazie*, 352(2), 1800292. <https://doi.org/10.1002/ardp.201800292>.
- Hamad, A., Abbas Khan, M., Ahmad, I., Imran, A., Khalil, R., Al-Adhami, T., Miraz Rahman, K., Quratlain, Zahra, N., & Shafiq, Z. (2020). Probing sulphamethazine and sulphamethoxazole based Schiff bases as urease inhibitors; synthesis, characterization, molecular docking and ADME evaluation. *Bioorganic Chemistry*, 105, 104336. <https://doi.org/10.1016/j.bioorg.2020.104336>.
- Han, W., & Li, C. (2010). Linking type 2 diabetes and Alzheimer's disease. *Proceedings of the National Academy of Sciences*, 107(15), 6557–6558. <https://doi.org/10.1073/pnas.1002555107>.
- Hollander, P. (1992). Safety profile of acarbose, an α -glucosidase inhibitor. *Drugs*, 44(3), 47–53. <https://doi.org/10.2165/00003495-199200443-00007>.
- Iftikhar, M., Saleem, M., Riaz, N., Ahmed, I., Rahman, J., Ashraf, M., Sharif, M. S., Khan, S. U., & Htar, T. T. (2019). A novel five-step synthetic route to 1, 3, 4-oxadiazole derivatives with potent α -glucosidase inhibitory potential and their in silico studies. *Archiv Der Pharmazie*, 352(12), 1900095. <https://doi.org/10.1002/ardp.201900095>.
- Işık, M. (2019). The binding mechanisms and inhibitory effect of intravenous anesthetics on AChE in vitro and in vivo: Kinetic analysis and molecular docking. *Neurochemical Research*, 44(9), 2147–2155. <https://doi.org/10.1007/s11064-019-02852-y>.
- Işık, M., Akocak, S., Lolak, N., Taslimi, P., Türkeş, C., Gülçin, İ., Durgun, M., & Beydemir, Ş. (2020a). Synthesis, characterization, biological evaluation, and in silico studies of novel 1,3-diaryltriazene-substituted sulfathiazole derivatives. *Archiv Der Pharmazie*, 353(9), e2000102. <https://doi.org/10.1002/ardp.202000102>.
- Işık, M., Beydemir, Ş., Demir, Y., Durgun, M., Türkeş, C., Nasır, A., Necip, A., & Akkuş, M. (2020b). Benzenesulfonamide derivatives containing imine and amine groups: Inhibition on human paraoxonase and molecular docking studies. *International Journal of Biological Macromolecules*, 146, 1111–1123. <https://doi.org/10.1016/j.ijbiomac.2019.09.237>.
- Işık, M., Beydemir, Ş., Yılmaz, A., Naldan, M. E., Aslan, H. E., & Gülçin, İ. (2017). Oxidative stress and mRNA expression of acetylcholinesterase in the leukocytes of ischemic patients. *Biomedicine & Pharmacotherapy*, 87, 561–567. <https://doi.org/10.1016/j.biopha.2017.01.003>.
- Işık, M., Demir, Y., Durgun, M., Türkeş, C., Necip, A., & Beydemir, Ş. (2020c). Molecular docking and investigation of 4-(benzylideneamino)- and 4-(benzylamino)-benzenesulfonamide derivatives as potent AChE inhibitors. *Chemical Papers*, 74, 1395–1405. <https://doi.org/10.1007/s11696-019-00988-3>.
- Istrefi, Q., Türkeş, C., Arslan, M., Demir, Y., Nixha, A. R., Beydemir, Ş., & Küfreviođlu, Ö. İ. (2020). Sulfonamides incorporating ketene N, S-acetal bioisosteres as potent carbonic anhydrase and acetylcholinesterase inhibitors. *Archiv Der Pharmazie*, 353(6), 1900383. <https://doi.org/10.1002/ardp.201900383>.
- Kalaycı, M., Türkeş, C., Arslan, M., Demir, Y., & Beydemir, Ş. (2021). Novel benzoic acid derivatives: Synthesis and biological evaluation as multi-target acetylcholinesterase and carbonic anhydrase inhibitors. *Archiv Der Pharmazie*, 354(3), e2000282. <https://doi.org/10.1002/ardp.202000282>.
- Kessler, P., Marchot, P., Silva, M., & Servent, D. (2017). The three-finger toxin fold: A multifunctional structural scaffold able to modulate cholinergic functions. *Journal of Neurochemistry*, 142, 7–18. <https://doi.org/10.1111/jnc.13975>.
- Khanfar, M. A., AbuKhadher, M. M., Alqtaishat, S., & Taha, M. O. (2013). Pharmacophore modeling, homology modeling, and in silico screening reveal mammalian target of rapamycin inhibitory activities for sotalol, glyburide, metipranolol, sulfamethizole, glipizide, and pioglitazone. *Journal of Molecular Graphics and Modelling*, 42, 39–49. <https://doi.org/10.1016/j.jmgm.2013.02.009>.
- Kilic, A., Beyazsakal, L., Işık, M., Türkeş, C., Necip, A., Takım, K., & Beydemir, Ş. (2020). Mannich reaction derived novel boron complexes with amine-bis (phenolate) ligands: Synthesis, spectroscopy and in vitro/in silico biological studies. *Journal of Organometallic Chemistry*, 927, 121542. <https://doi.org/10.1016/j.jorgchem.2020.121542>.
- Kosak, U., Brus, B., Knez, D., Zakelj, S., Trontelj, J., Pislar, A., Sink, R., Jukic, M., Zivin, M., & Podkova, A. (2018). The magic of crystal structure-based inhibitor optimization: Development of a butyrylcholinesterase inhibitor with picomolar affinity and in vivo activity. *Journal of Medicinal Chemistry*, 61(1), 119–139. <https://doi.org/10.1021/acs.jmedchem.7b01086>.
- Krieger, R. (2010). *Hayes' handbook of pesticide toxicology*. Academic Press.
- Lipinski, C. A., Lombardo, F., Dominy, B. W., & Feeney, P. J. (1997). Experimental and computational approaches to estimate solubility and permeability in drug discovery and development settings. *Advanced Drug Delivery Reviews*, 23(1–3), 3–25. [https://doi.org/10.1016/S0169-409X\(96\)00423-1](https://doi.org/10.1016/S0169-409X(96)00423-1).
- Lolak, N., Akocak, S., Türkeş, C., Taslimi, P., Işık, M., Beydemir, Ş., Gülçin, İ., & Durgun, M. (2020). Synthesis, characterization, inhibition effects, and molecular docking studies as acetylcholinesterase, α -glucosidase, and carbonic anhydrase inhibitors of novel benzenesulfonamides incorporating 1, 3, 5-triazine structural motifs. *Bioorganic Chemistry*, 100, 103897. <https://doi.org/10.1016/j.bioorg.2020.103897>.
- Lou, Y., McDonald, P. C., Oloumi, A., Chia, S., Ostlund, C., Ahmadi, A., Kyle, A., Auf Dem Keller, U., Leung, S., & Huntsman, D. (2011). Targeting tumor hypoxia: Suppression of breast tumor growth and metastasis by novel carbonic anhydrase IX inhibitors. *Cancer Research*, 71(9), 3364–3376. <https://doi.org/10.1158/0008-5472.CAN.10-4261>.
- McCulloch, D. K., Kurtz, A. B., & Tattersall, R. B. (1983). A new approach to the treatment of nocturnal hypoglycemia using alpha-glucosidase inhibition. *Diabetes Care*, 6(5), 483–487. <https://doi.org/10.2337/diacare.6.5.483>.
- Mughal, E. U., Javid, A., Sadiq, A., Murtaza, S., Zafar, M. N., Khan, B. A., Sumrra, S. H., Tahir, M. N., & Khan, K. M. (2018). Synthesis, structure-activity relationship and molecular docking studies of 3-O-flavonol glycosides as cholinesterase inhibitors. *Bioorganic & Medicinal Chemistry*, 26(12), 3696–3706. <https://doi.org/10.1016/j.bmc.2018.05.050>.
- Mughal, E. U., Sadiq, A., Ashraf, J., Zafar, M. N., Sumrra, S. H., Tariq, R., Mumtaz, A., Javid, A., Khan, B. A., & Ali, A. (2019). Flavonols and 4-thioflavonols as potential acetylcholinesterase and butyrylcholinesterase inhibitors: Synthesis, structure-activity relationship and molecular docking studies. *Bioorganic Chemistry*, 91, 103124. <https://doi.org/10.1016/j.bioorg.2019.103124>.
- Mughal, E. U., Sadiq, A., Ayub, M., Naeem, N., Javid, A., Sumrra, S. H., Zafar, M. N., Khan, B. A., Malik, F. P., & Ahmed, I. (2020). Exploring 3-Benzyloxyflavones as new lead cholinesterase inhibitors: Synthesis, structure-activity relationship and molecular modelling simulations. *Journal of Biomolecular Structure and Dynamics*, 1–14. <https://doi.org/10.1080/07391102.2020.1803136>.
- Mughal, E. U., Sadiq, A., Murtaza, S., Rafique, H., Zafar, M. N., Riaz, T., Khan, B. A., Hameed, A., & Khan, K. M. (2017). Synthesis, structure-activity relationship and molecular docking of 3-oxoaurones and 3-thioaurones as acetylcholinesterase and butyrylcholinesterase inhibitors. *Bioorganic & Medicinal Chemistry*, 25(1), 100–106. <https://doi.org/10.1016/j.bmc.2016.10.016>.
- Nachon, F., Carletti, E., Ronco, C., Trovaslet, M., Nicolet, Y., Jean, L., & Renard, P.-Y. (2013). Crystal structures of human cholinesterases in complex with huprine W and tacrine: Elements of specificity for anti-Alzheimer's drugs targeting acetyl- and butyryl-cholinesterase. *Biochemical Journal*, 453(3), 393–399. <https://doi.org/10.1042/BJ20130013>.
- Nakagawa, K. (2013). Studies targeting α -glucosidase inhibition, antiangiogenic effects, and lipid modification regulation: Background, evaluation, and challenges in the development of food ingredients for

- therapeutic purposes. *Bioscience, Biotechnology, and Biochemistry*, 77(5), 900–908. <https://doi.org/10.1271/bbb.120908>.
- Pacchiano, F., Carta, F., McDonald, P. C., Lou, Y., Vullo, D., Scozzafava, A., Dedhar, S., & Supuran, C. T. (2011). Ureido-substituted benzenesulfonamides potently inhibit carbonic anhydrase IX and show antimetastatic activity in a model of breast cancer metastasis. *Journal of Medicinal Chemistry*, 54(6), 1896–1902. <https://doi.org/10.1021/jm101541x>.
- Pohanka, M. (2012). Acetylcholinesterase inhibitors: A patent review (2008–present). *Expert Opinion on Therapeutic Patents*, 22(8), 871–886. <https://doi.org/10.1517/13543776.2012.701620>.
- Poulsen, K. A., Andersen, E. C., Hansen, C. F., Klausen, T. K., Hougaard, C., Lambert, I. H., & Hoffmann, E. K. (2010). Deregulation of apoptotic volume decrease and ionic movements in multidrug-resistant tumor cells: Role of chloride channels. *American Journal of Physiology-Cell Physiology*, 298(1), C14–C25. <https://doi.org/10.1152/ajpcell.00654.2008>.
- Provensi, G., Passani, M. B., Costa, A., Izquierdo, I., & Blandina, P. (2020). Neuronal histamine and the memory of emotionally salient events. *British Journal of Pharmacology*, 177(3), 557–569. <https://doi.org/10.1111/bph.14476>.
- Rao, A. A., Sridhar, G. R., & Das, U. N. (2007). Elevated butyrylcholinesterase and acetylcholinesterase may predict the development of type 2 diabetes mellitus and Alzheimer's disease. *Medical Hypotheses*, 69(6), 1272–1276. <https://doi.org/10.1016/j.mehy.2007.03.032>.
- Reale, M., Costantini, E., Di Nicola, M., D'Angelo, C., Franchi, S., D'Aurora, M., Di Bari, M., Orlando, V., Galizia, S., & Ruggieri, S. (2018). Butyrylcholinesterase and Acetylcholinesterase polymorphisms in Multiple Sclerosis patients: Implication in peripheral inflammation. *Scientific Reports*, 8(1), 1–9. <https://doi.org/10.1038/s41598-018-19701-7>.
- Ren, S., Xu, D., Pan, Z., Gao, Y., Jiang, Z., & Gao, Q. (2011). Two flavanone compounds from litchi (*Litchi chinensis* Sonn.) seeds, one previously unreported, and appraisal of their α -glucosidase inhibitory activities. *Food Chemistry*, 127(4), 1760–1763. <https://doi.org/10.1016/j.foodchem.2011.02.054>.
- Roig-Zamboni, V., Cobucci-Ponzano, B., Iacono, R., Ferrara, M. C., Germany, S., Bourne, Y., Parenti, G., Moracci, M., & Sulzenbacher, G. (2017). Structure of human lysosomal acid α -glucosidase—a guide for the treatment of Pompe disease. *Nature Communications*, 8(1), 1–10. <https://doi.org/10.1038/s41467-017-01263-3>.
- Ruivo, L. M. T.-G., Baker, K. L., Conway, M. W., Kinsley, P. J., Gilmour, G., Phillips, K. G., Isaac, J. T., Lowry, J. P., & Mellor, J. R. (2017). Coordinated acetylcholine release in prefrontal cortex and hippocampus is associated with arousal and reward on distinct timescales. *Cell Reports*, 18(4), 905–917. <https://doi.org/10.1016/j.celrep.2016.12.085>.
- Saha, T., Hossain, M. S., Saha, D., Lahiri, M., & Talukdar, P. (2016). Chloride-mediated apoptosis-inducing activity of bis (sulfonamide) anionophores. *Journal of the American Chemical Society*, 138(24), 7558–7567. <https://doi.org/10.1021/jacs.6b01723>.
- Saleem, F., Khan, K. M., Chigurupati, S., Solangi, M., Nemala, A. R., Mushtaq, M., Ul-Haq, Z., Taha, M., & Perveen, S. (2021). Synthesis of azachalcones, their α -amylase, α -glucosidase inhibitory activities, kinetics, and molecular docking studies. *Bioorganic Chemistry*, 106, 104489. <https://doi.org/10.1016/j.bioorg.2020.104489>.
- Sastry, G. M., Adzhigirey, M., Day, T., Annabhimoju, R., & Sherman, W. (2013). Protein and ligand preparation: Parameters, protocols, and influence on virtual screening enrichments. *Journal of Computer-Aided Molecular Design*, 27(3), 221–234. <https://doi.org/10.1007/s10822-013-9644-8>.
- Schneider, L. S. (2000). A critical review of cholinesterase inhibitors as a treatment modality in Alzheimer's disease. *Dialogues in Clinical Neuroscience*, 2(2), 111. <https://doi.org/10.31887/DCNS.2000.2.2/lschneider>.
- Sever, B., Altıntop, M. D., Demir, Y., Türkes, C., Özbaş, K., Çiftçi, G. A., Beydemir, Ş., & Özdemir, A. (2021). A new series of 2,4-thiazolidinediones endowed with potent aldose reductase inhibitory activity. *Open Chemistry*, 19, 347–357. <https://doi.org/10.1515/chem-2021-0032>.
- Sever, B., Türkes, C., Altıntop, M. D., Demir, Y., & Beydemir, Ş. (2020). Thiazolyl-pyrazoline derivatives: In vitro and in silico evaluation as potential acetylcholinesterase and carbonic anhydrase inhibitors. *International Journal of Biological Macromolecules*, 163, 1970–1988. <https://doi.org/10.1016/j.jbiomac.2020.09.043>.
- Shelley, J. C., Chollet, A., Frye, L. L., Greenwood, J. R., Timlin, M. R., & Uchimaya, M. (2007). Epik: A software program for pK a prediction and protonation state generation for drug-like molecules. *Journal of Computer-Aided Molecular Design*, 21(12), 681–691. <https://doi.org/10.1007/s10822-007-9133-z>.
- Supuran, C. T., Scozzafava, A., Jurca, B. C., & Ilies, M. A. (1998). Carbonic anhydrase inhibitors-Part 49: Synthesis of substituted ureido and thio-ureido derivatives of aromatic/heterocyclic sulfonamides with increased affinities for isozyme I. *European Journal of Medicinal Chemistry*, 33(2), 83–93. [https://doi.org/10.1016/S0223-5234\(98\)80033-0](https://doi.org/10.1016/S0223-5234(98)80033-0).
- Taha, M., Imran, S., Salahuddin, M., Iqbal, N., Rahim, F., Uddin, N., Shehzad, A., Khalid Farooq, R., Alomari, M., & Mohammed Khan, K. (2021). Evaluation and docking of indole sulfonamide as a potent inhibitor of α -glucosidase enzyme in streptozotocin-induced diabetic albino wistar rats. *Bioorganic Chemistry*, 110, 104808. <https://doi.org/10.1016/j.bioorg.2021.104808>.
- Taslimi, P., Caglayan, C., Farzaliyev, V., Nabiyev, O., Sujayev, A., Turkan, F., Kaya, R., & Gulcin, İ. (2018). Synthesis and discovery of potent carbonic anhydrase, acetylcholinesterase, butyrylcholinesterase, and α -glucosidase enzymes inhibitors: The novel N, N'-bis-cyanomethylamine and alkoxyethylamine derivatives. *Journal of Biochemical and Molecular Toxicology*, 32(4), e22042. <https://doi.org/10.1002/jbt.22042>.
- Taslimi, P., Işık, M., Türkan, F., Durgun, M., Türkes, C., Gülçin, İ., & Beydemir, Ş. (2020a). Benzenesulfonamide derivatives as potent acetylcholinesterase, α -glycosidase, and glutathione S-transferase inhibitors: Biological evaluation and molecular docking studies. *Journal of Biomolecular Structure and Dynamics*, 1–12. <https://doi.org/10.1080/07391102.2020.1790422>.
- Taslimi, P., Turhan, K., Türkan, F., Karaman, H. S., Turgut, Z., & Gulcin, I. (2020b). Cholinesterases, α -glycosidase, and carbonic anhydrase inhibition properties of 1H-pyrazolo [1, 2-b] phthalazine-5, 10-dione derivatives: Synthetic analogues for the treatment of Alzheimer's disease and diabetes mellitus. *Bioorganic Chemistry*, 97, 103647. <https://doi.org/10.1016/j.bioorg.2020.103647>.
- Topal, F. (2019a). Inhibition profiles of Voriconazole against acetylcholinesterase, α -glycosidase, and human carbonic anhydrase I and II isoenzymes. *Journal of Biochemical and Molecular Toxicology*, 33(10), e22385. <https://doi.org/10.1002/jbt.22385>.
- Topal, M. (2019b). The inhibition profile of sesamol against α -glycosidase and acetylcholinesterase enzymes. *International Journal of Food Properties*, 22(1), 1527–1535. <https://doi.org/10.1080/10942912.2019.1656234>.
- Tugrak, M., Gul, H. I., Demir, Y., & Gulcin, I. (2020). Synthesis of benzamide derivatives with thiourea-substituted benzenesulfonamides as carbonic anhydrase inhibitors. *Archiv Der Pharmazie*, 354(2), e2000230. <https://doi.org/10.1002/ardp.202000230>.
- Turhan, K., Pektaş, B., Türkan, F., Tuğcu, F. T., Turgut, Z., Taslimi, P., Karaman, H. S., & Gulcin, I. (2020). Novel benzo [b] xanthene derivatives: Bismuth (III) triflate-catalyzed one-pot synthesis, characterization, and acetylcholinesterase, glutathione S-transferase, and butyrylcholinesterase inhibitory properties. *Archiv Der Pharmazie*, 353(8), 2000030. <https://doi.org/10.1002/ardp.202000030>.
- Turkan, F., Cetin, A., Taslimi, P., Karaman, H. S., & Gulcin, İ. (2019). Synthesis, characterization, molecular docking and biological activities of novel pyrazoline derivatives. *Archiv Der Pharmazie*, 352(6), 1800359. <https://doi.org/10.1002/ardp.201800359>.
- Türkes, C. (2019a). Investigation of potential paraoxonase-I inhibitors by kinetic and molecular docking studies: Chemotherapeutic drugs. *Protein and Peptide Letters*, 26(6), 392–402. <https://doi.org/10.2174/0929866526666190226162225>.
- Türkes, C. (2019b). A potential risk factor for paraoxonase 1: In silico and in-vitro analysis of the biological activity of proton-pump inhibitors. *Journal of Pharmacy and Pharmacology*, 71(10), 1553–1564. <https://doi.org/10.1111/jphp.13141>.
- Türkes, C., Arslan, M., Demir, Y., Cocaj, L., Nixha, A. R., & Beydemir, Ş. (2019a). Synthesis, biological evaluation and in silico studies of novel

- N-substituted phthalazine sulfonamide compounds as potent carbonic anhydrase and acetylcholinesterase inhibitors. *Bioorganic Chemistry*, 89, 103004. <https://doi.org/10.1016/j.bioorg.2019.103004>.
- Türkeş, C., & Beydemir, Ş. (2020). Inhibition of human serum paraoxonase-I with antimycotic drugs: In vitro and in silico studies. *Applied Biochemistry and Biotechnology*, 190(1), 252–269. <https://doi.org/10.1007/s12010-019-03073-3>.
- Türkeş, C., Beydemir, Ş., & Küfrevioğlu, Ö. İ. (2019b). In vitro and in silico studies on the toxic effects of antibacterial drugs as human serum paraoxonase 1 inhibitor. *ChemistrySelect*, 4(33), 9731–9736. <https://doi.org/10.1002/slct.201902424>.
- Türkeş, C., Demir, Y., & Beydemir, S. (2019c). Anti-diabetic properties of calcium channel blockers: Inhibition effects on aldose reductase enzyme activity. *Applied Biochemistry and Biotechnology*, 189(1), 318–329. <https://doi.org/10.1007/s12010-019-03009-x>.
- Türkeş, C., Demir, Y., & Beydemir, Ş. (2020). Some calcium-channel blockers: Kinetic and in silico studies on paraoxonase-I. *Journal of Biomolecular Structure and Dynamics*, 1–9. <https://doi.org/10.1080/07391102.2020.1806927>.
- Türkeş, C., Demir, Y., & Beydemir, Ş. (2021). Calcium channel blockers: Molecular docking and inhibition studies on carbonic anhydrase I and II isoenzymes. *Journal of Biomolecular Structure and Dynamics*, 39(5), 1672–1680. <https://doi.org/10.1080/07391102.2020.1736631>.
- Türkeş, C., Söyüt, H., & Beydemir, Ş. (2014). Effect of calcium channel blockers on paraoxonase-1 (PON1) activity and oxidative stress. *Pharmacological Reports*, 66(1), 74–80. <https://doi.org/10.1016/j.pharep.2013.08.007>.
- Türkeş, C., Söyüt, H., & Beydemir, Ş. (2015). Human serum paraoxonase-1 (hPON1): In vitro inhibition effects of moxifloxacin hydrochloride, levofloxacin hemihydrate, cefepime hydrochloride, cefotaxime sodium and ceftizoxime sodium. *Journal of Enzyme Inhibition and Medicinal Chemistry*, 30(4), 622–628. <https://doi.org/10.3109/14756366.2014.959511>.
- Türkeş, C., Söyüt, H., & Beydemir, Ş. (2016). In vitro inhibitory effects of palonosetron hydrochloride, bevacizumab and cyclophosphamide on purified paraoxonase-I (hPON1) from human serum. *Environmental Toxicology and Pharmacology*, 42, 252–257. <https://doi.org/10.1016/j.etap.2015.11.024>.
- Yu, X.-H., Hong, X.-Q., Mao, Q.-C., & Chen, W.-H. (2019). Biological effects and activity optimization of small-molecule, drug-like synthetic anion transporters. *European Journal of Medicinal Chemistry*, 184, 111782. <https://doi.org/10.1016/j.ejmech.2019.111782>.
- Zaman, M., Khan, A. N., Zakariya, S. M., & Khan, R. H. (2019). Protein misfolding, aggregation and mechanism of amyloid cytotoxicity: An overview and therapeutic strategies to inhibit aggregation. *International Journal of Biological Macromolecules*, 134, 1022–1037. <https://doi.org/10.1016/j.ijbiomac.2019.05.109>.